Article

Computer Science Techniques Applied to Temperature Control in Biodiesel Production: Mathematical Modeling, Optimization, and Sensorless Technique

Mario C. Maya-Rodriguez [1] , **Ignacio Carvajal-Mariscal** [1,*] , **Raúl López-Muñoz** [2,*] , **Mario A. Lopez-Pacheco** [1] and **René Tolentino-Eslava** [1]

[1] Escuela Superior de Ingeniería Mecánica y Eléctrica Unidad Zacatenco, Instituto Politécnico Nacional, Mexico City 07738, Mexico; mmayar@ipn.mx (M.C.M.-R.); mlaopezp@ipn.mx (M.A.L.-P.); rtolentino@ipn.mx (R.T.-E.)

[2] Unidad Profesional Interdisciplinaria en Ingeniería y Tecnologías Avanzadas (UPIITA), Instituto Politécnico Nacional, Mexico City 07340, Mexico

[*] Correspondence: icarvajal@ipn.mx (I.C.-M.); raulopezm@ipn.mx (R.L.-M.)

Abstract: This paper demonstrates that biodiesel production processes can be optimized through implementing a controller based on fuzzy logic and neural networks. The system dynamics are identified utilizing convolutional neural networks, enabling tests of the reactor temperature response under different control law proposals. In addition, a sensorless technique using a convolutional neural network to replace the sensor/transmitter signal in case of failure is implemented. Two optimization functions are proposed utilizing a metaheuristic algorithm based on differential evolution, where the aim is to minimize the use of cooling for the control of the reactor temperature. Finally, the control system proposals are compared, and the results show that a neuro-fuzzy controller without optimization restrictions generated unviable ITAE (1.9597×10^7) and TVU (22.3993) performance metrics, while the restriction proposed in this work managed to minimize these metrics, improving both the ITAE (3.3928×10^6) and TVU (17.9132). These results show that combining the sensorless technique and our optimization method for the cooling stage enables energy saving in the temperature control processes required for biodiesel production.

Keywords: control process; biodiesel; optimization; sensorless technique

1. Introduction

It is important for industrial control systems to maximize profits and the use of resources in their production processes in order to remain competitive. To achieve this, it is necessary to optimize different areas, such as Electricity, Electronics, Mechanics, Administration, and Automatic Control, among others. In the area of Automatic Control, it is possible to contribute to the fulfillment of the optimization objective in the following ways: (1) tuning classical controllers [1]; (2) modeling and identification of parameters [2]; (3) monitoring and prediction of behaviors [3]; and (4) implementation of non-conventional controllers [4]. This work will focus on the modeling and identification of parameters, allowing a mathematical expression of the linear or nonlinear nature of production processes through the application of classical mechanics methods and computer science techniques [2]. As a possible benefit, it is possible to carry out simulations of the behavior and dynamics of a process under different considerations such as operating conditions, different controllers, and performance evaluation, among others. This has to do with purposes associated with the design of production plants as well as with the optimization of already established

production processes. The implementation of non-conventional controllers is increasing worldwide and will be seen with greater force in the industry of undeveloped countries, because most of them use classical controllers. Due to the complex nature of these processes, classical controllers quickly reach their limitations and affect the profits of a factory over time through, for example, using more energy than necessary, product quality problems, and difficulty in complying with environmental regulations, among other issues. Controllers based on expert systems with fuzzy logic and those based on neural networks have gained popularity in recent years [5]. However, this type of controller has a fundamental problem—the inherent dependence on hyper-parameters and their initial conditions—as well as the classic problems of stability and convergence. Given the rapprochement between Automatic Control and Computer Science in the last few decades, it is now possible to combine the techniques and reach the optimization objective from a metaheuristics point of view, minimizing the dependence on the selection of initial conditions. Mexico's energy consumption is primarily distributed to the transportation sector as well as heat and electricity generation. All this energy comes from fossil material burning (approximately 60%) [6], renewable sources (9%), and biodiesel (5%) [7], among other sources. Several political reforms in Mexico have been implemented to reduce the pollutant emissions into the atmosphere. Although 35% of the total energy production came from renewable resources by the end of 2024, several factors limited this progress [8], such as high production costs, inadequate infrastructure for the energy production, and the lack of incentives to develop those products [9]. However, biodiesel production has prospered thanks to various recent research studies on its production and its promotion in different applications [6,10,11].

Biodiesel production requires a specific viscosity similar to that of diesel, which is achieved by mixing different substances and heating them under particular conditions for each type of mixture in transesterification reactors [12]. Adequate control of the inside of the reactor, specifically temperature control, is important. Nowadays, most of the theoretical advances in the area of Automatic Control are not being effectively exploited mainly for two reasons. The first reason is due to a lack of collaboration with areas of industrial production, which need to contribute their perspective in order to guarantee the efficient use of resources, as well as the problems and requirements for national growth. The second reason is due to the lack of interest or efforts by researchers to carry out implementations in real-world problems, which sometimes, depending on the observer, are underestimated. However, the union of both aspects will allow us to continue developing and finding ways to achieve industrialization objectives, the optimization of resources, and the satisfaction of human needs in accordance with the corresponding area in question. In this work, an illustration of the above is proposed by combining a problem of interest, such as the generation of biodiesel, convolutional neural networks, metaheuristic algorithms, and control through a neuro-fuzzy approach. One can find works such as [13], where a comparative test of a boiler is presented, proving the maximum boiler efficiency indicators and also the minimum toxicity of exhaust gases discharged into the atmosphere, all this considering the proposed control system.

An important part of the control area is the identification of the system to be controlled, because most control techniques used in the industry require a model to be applied [4]. In a real-world system, to obtain a model from them requires a lot of variables, such as knowledge of the system, physical and environmental conditions, and the type of model to be used, i.e., linear, nonlinear, parametric, non-parametric, continuous or discrete time, among others [14]. The aim of these models is to represent in the best way possible the real system and to be as simple as possible, too. Different techniques of modeling have been developed through the years, each one trying to satisfy a specific need [15]. For example, [16] represents the issues that nonlinear systems could introduce in the modeling

process and the excitation signals type that could be used in these systems. Also, in [17], linear models were not enough to capture all the neural activity and relationships in the neural system, so they propose a nonlinear model that helps in this matter and also produces sensitive biomarkers to improve diagnosis in neurological disorders. In [18], they propose the use of neural networks as a modeling method for a nonlinear system with constraints on states, which is paired with a back-stepping algorithm and an intelligent controller.

Neural networks use has drastically increased in the past twenty years with a variety of applications like object recognition [19], prediction [20,21], parametric estimation [22,23] and system control [24]. One of the most popular algorithms within the neural networks is the convolutional neural network (CNN) [25], inspired by the studies of Hubel and Wiesel in the 1950s of the visual processing system of animals [26], and image classification is its main application [27]. A recent deep study of recent advances in the use of CNNs can be found in [28,29], where many modified architectures to specific applications of CNNs are gathered together. As regards system identification using CNNs, Guodong Fan and Xi Zhang present an architecture of CNNs to estimate battery capacity using voltage data from different degradation levels [30]. In [31], a CNN is employed for the rapid prediction of fluvial flood inundation where hydraulic/hydrodynamic models used for this same propose are too computationally demanding. Another technique that can be applied to the identification of systems is sensorless, which has been gaining popularity in pump, motor, fan, and extractor control systems, among others [32]. Since sometimes it is not possible to carry out the measurement of certain variables due to their complexity or a high implementation cost, the estimation and approximation of the variables have an inherent and strong correlation with the identification of a mathematical model and its parameters. It is possible to obtain benefits for the prediction of the behavior of a system or to replace a primary and secondary element (sensor/transmitter) due to an instrument failure or communication failure. The implementation of this type of techniques can help reduce instrumentation costs and avoid unscheduled shutdowns due to instrument replacement; however, this should not be used under any circumstances for security systems.

In [33–35], a variety of works have addressed the tuning of different controllers through experimentation, using random combinations, leaving aside hard optimization problems. According to [36], a neuro-fuzzy controller (NFC) controller is a hybridization between controllers based on fuzzy networks [37,38] and neural networks based on [39]. A fuzzy logic system uses if–then rules to determine the appropriate course of action based on input data. The programmer, using its expertise, initially proposes these rules and is further refined by means of a machine learning algorithm. The rules are based not only on the experience of the programmer but on how the system learns from the data. This process involves tuning the hyper-parameters of the neural network and the elements associated with the inference laws of fuzzy logic. Metaheuristics algorithms provide solutions for optimization problems when analytical or classical methods are not available. This non-viability mainly occurs if the objective function to be optimized is not derivable or when the computing resources for analytical methods are limited.

The main objectives of this work are presented below:

- To identify the dynamics of a biodiesel production system by means of a CNN.
- To tune a neuro-fuzzy controller by applying metahumanistic techniques using the system obtained by means of the CNN.
- To propose the cooling action as a temperature control problem to optimize the energy applied in this stage.
- To apply a sensorless technique based on the implementation of a CNN for the replacement of the control signal in case of failure.

Biodiesel production systems present challenges and obstacles associated with various areas of engineering. Computer science techniques can be used to enhance topics related to Automatic Control, such as artificial neural networks and optimization methods. This work presents solutions to different problems featuring a mathematical model to perform the tuning of the temperature control based on convolutional neural networks and tuning for an NFC counter based on an optimization problem defined from the control objective to minimize the heating stage by means of metaheuristics. In addition, a sensorless technique is implemented in case of failure of the sensor/transmitter element, which consists of using a convolutional neural network to momentarily replace the original signal of the system and avoid problems in the production process. Finally, the result is a model that allows simulations to be carried out to observe the dynamics of the process and thereby evaluate the production process. A method is also proposed for energy saving by minimizing the use of the cooling stage and, finally, a sensorless technique to guarantee the continuity of the production process in the event of sensor/transmitter failure.

2. Materials and Methods

2.1. Problem Description

One of the great challenges in the application of Automatic Control in the industry is the need to carry out tests of the controllers virtually and to allow the evaluation of the effectiveness of the control law through measurements or performance metrics. However, a method based on trial and error is not economically feasible in most cases due to the time it may take and the inputs or raw materials required to carry out such tests. To work virtually, it is necessary to have a dynamic mathematical model that allows emulation of the behavior of the process in a specialized software environment and, from there, to carry out dynamic tests under a specific control proposal to achieve the control objectives based on the need to optimize the industrial process. Determining a mathematical model of an industrial production process is often highly complex and complicated by means of laws based on classical mechanics to obtain the differential equations that describe its behavior over time. One way that has emerged to try to solve this problem is the use of parametric and non-parametric identification techniques, which allow the approximation of dynamics or parameters by means of the input and output signals of a process. In general, industrial processes have nonlinear behaviors, which implies an important challenge to determine a mathematical structure that describes their behavior. One of the most used techniques to determine their dynamics is artificial neural networks; due to their plasticity and flexibility in the learning process, they become strong candidates to be used since in industrial processes, it is possible to collect a large amount of information on the control action (manipulated variable) and the process variable (controlled variable) through a data acquisition system. The system presented in [40] is taken as a case study, which is described through Figure 1, where TC, T_p, T_1 represents the thermal agent temperature, output product temperature and the temperature of the product, respectively. The objective of control is to regulate the temperature of the product (T_1) as close to the reference temperature T_0 as possible. We control the action on the manipulated variable (valve), determined by the control law programmed in the control system, using the information from the temperature variable transducer coming from the reactor. Also, the flow of cold water and steam to the tank is controlled in order to reach the desired temperature. Here, q_{ar} is the heat of the cold water, q_p is the output product heat and q_{ab} is the steam heat. The detailed description of the physical–chemical process that takes place in the production of biodiesel and the mathematical model can be found in [40].
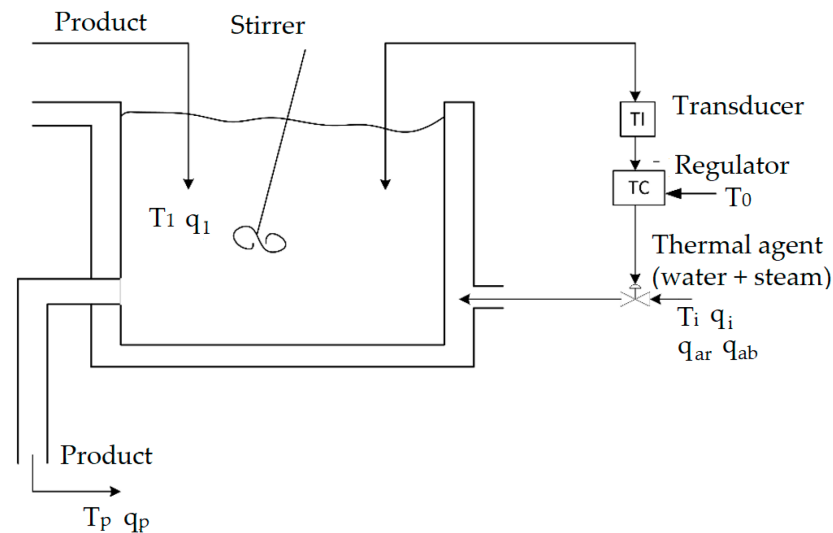
Figure 1. Pilot plant scheme [40].

The transfer function for the tank temperature is described by (1), according to [40]:

$$G_f = \frac{4}{(360s + 1)(1143s + 1)}. \tag{1}$$

To obtain (1), a cascade of three other transfer functions is needed, i.e., $G_f = G_E G_p G_T$, where these functions represent the dynamic and the static part of the complete system, which is shown next:

$$G_E = \frac{K_E}{T_E s + 1}; \tag{2}$$

$$G_P = \frac{K_p}{T_p s + 1}; \tag{3}$$

$$G_T = 2. \tag{4}$$

The execution element is represented by (2), where $K_E = 2$ and $T_E = 360$; (3) applies to the process with $T_p = 1143\,s$, $K_p = 1$, and for the temperature transducer, (4) is used as a gain. These three transfer functions, working together, ensure the temperature of the tank remains at the same level as long as the vegetable oil and the methanol react with each other and the fatty acids methyl ester and glycerin are produced in the correct way. Although model (1) represents a mathematical model of the system by means of differential equations expressed in the frequency domain through a transfer function, it is worth mentioning that it is a linear approximation that is invariant in time and with initial conditions equal to zero. No model can be an exact copy of the system, so the general considerations that are made to obtain the dynamics of the system generate uncertainty, and therefore, a controller based on that model naturally has problems in the experimental phase. Moreover, the parameters of a mathematical model are time-variant either because of environmental conditions or due to the properties of the system itself. In the case of biodiesel production, this may occur during the process. In the transesterification stage, it is possible to observe adverse phenomena within the equipment and instruments, such as residual material, gas emissions, and physical effects on the tank due to heating even within operating ranges, among other effects. These apparently simple things can cause parameter variation.

For the above reasons, it is preferable to determine the mathematical model of the system in another way. In this work, convolutional neural networks are used, since they have been proven to be an important and novel tool in the area of computer science due to their learning capabilities. To apply the identification process to industrial systems and

ensure that the information collected is reliable, it is necessary for the data acquisition system to adequately measure the information of the process variable and the control action according to Theorem 1 and Shannon–Nyquist frequency sampling.

Theorem 1. *The sample rate f_s must be greater than twice the highest frequency component of interest in the signal. This frequency is usually known as the Nyquist frequency f_N* [2]:

$$f_s > 2 * f_N. \tag{5}$$

2.2. Identification Theory Using Convolutional Neural Network

The theory necessary to perform the system identification based on CNN is presented below. As an estimation method for the system, a convolutional neural network has been employed with the following structure: one fully connected layer as the output layer and two convolutional layers one after the other, in which each convolutional layer has 10 hyper-parameter named filters, $F_\ell \in \Re^3$ for $\ell = 1, 2$, and a ReLU activation function is applied to all filters separately.

The output of the CNN $\hat{q}_p$ is the estimated output of the real system q_p, which is calculated below:

$$\hat{q}_p = N_W * \Theta \tag{6}$$

where N_W are the synaptic weights in the output layer and Θ is the input to this layer, while Θ is the concatenation of the second convolutional layer outputs $\theta 2$:

$$\Theta = \begin{bmatrix} \theta 2_1^T & \theta 2_2^T \cdots \theta 2_{10}^T \end{bmatrix}^T \tag{7}$$

each $\theta 2_i$ for $i = 1, 2, \cdots, 10$, is calculated as

$$\theta 2_i = \max(F_{2,i} \odot \theta 1_i, 0) \tag{8}$$

where (8) is the ReLU operation over the convolution, $\odot$, of the filter $F_{2,i}$ with the ith-output $\theta 1_i$ of the first convolutional layer.

These outputs $\theta 1_i$ are obtained as follows:

$$\theta 1_i = \max(F_{1,i} \odot u_N, 0) \tag{9}$$

where u_N is the input vector for the CNN. For the training of the CNN, the backpropagation algorithm is employed to update the hyper-parameters of the CNN, in this case, the synaptic weights N_W and the filters $F_{2,i}$ and $F_{1,i}$ [41]. The rules for updating the hyper-parameters for the synaptic weights are, in backward order,

$$N_W(k+1) = N_W(k) - \eta \frac{\partial J}{\partial N_W} \tag{10}$$

with k representing the iteration in which the hyper-parameters are updated, J is the objective function to be minimized, and $J = \frac{1}{2}(\hat{q}_p - q_p)^2$. For the ReLU activation function, the gradient through this operation can be calculated as

$$\frac{\partial \theta h_2}{\partial F_{h,i} \odot \theta h - 1_i} = F_{h,i} \odot \theta h - 1_i \tag{11}$$

with $h = 1, 2$ representing the convolutional layer of the structure, which in case of $h = 1$ $\theta h - 1$ corresponds to the input to the CNN, u_N. For filters $F_{h,i}$, the update rule is

$$\frac{\partial F_{h,i} \odot \theta h - 1_i}{\partial F_{h,i}} = (F_{h,i} \odot \theta h - 1_i) \odot \theta h - 1_i \tag{12}$$

2.3. System Identification Procedure

The procedure for the system identification is as follows: 12,000 input–output data from the model are generated, which are used as training information. These data were obtained while the system was in a closed-loop configuration. In Figure 2, the procedure is shown, where the control signal U and the tank temperature output signal q_p are used as input to the CNN to produce a estimate value of the tank temperature $\hat{q}_p$. This value is fed back into the CNN along with q_p as an estimation error to calculate the gradient descendant to update the hyper-parameters of the CNN. This process is completed step by step; we received data from the system in different instants of time, the estimation was calculated, and the CNN was calculated in each one of these iterations. The correct application of Theorem 1 was needed to guarantee that the acquired data from the temperature system were reliable. Sometimes, it is hard to determine the Nyquist frequency in real-world applications. Nevertheless, experimental tests can be carried out through a sinusoidal input signal. For variables such as temperature, the dynamics of these signals are usually slow, so its f_N usually is low, in the order of Hertz, which generates problems in finding or proposing a sampling frequency. In this work, through trial and error, 1 s is enough to appreciate changes in the dynamics of the system.
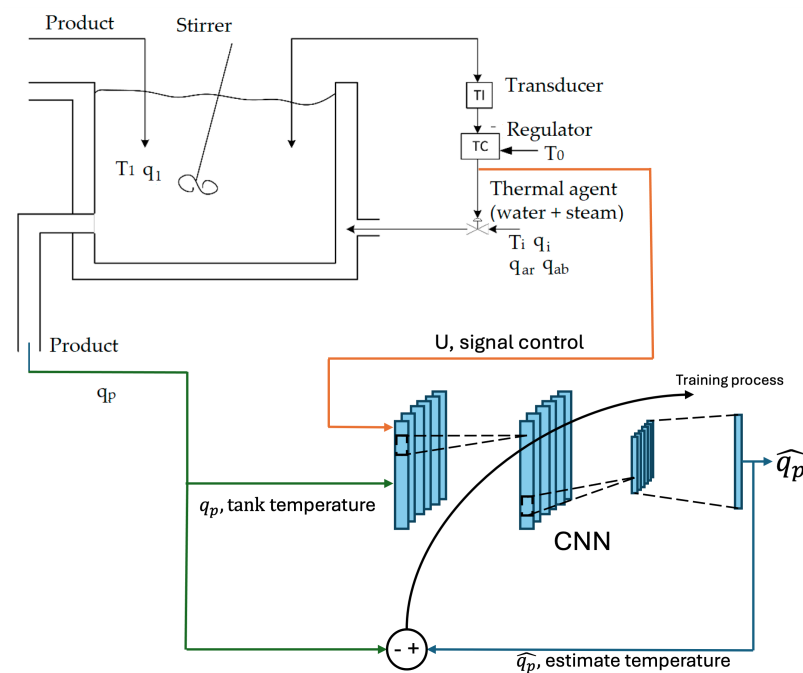

Figure 2. Identification procedure.

For the CNN, the vector u_N is generated in each iteration with the following structure:

$$u_N = \begin{bmatrix} U(k) & U(k-1) & \hat{q}_p(k-1) & \hat{q}_p(k-2) \end{bmatrix}^T \tag{13}$$

As a result of the system identification, Figure 3 shows these results, where both signals are practically equal, and the mean square error (MSE) metric was employed and has a measurement of the identification, leading to a value of 5.52×10^{-21}.
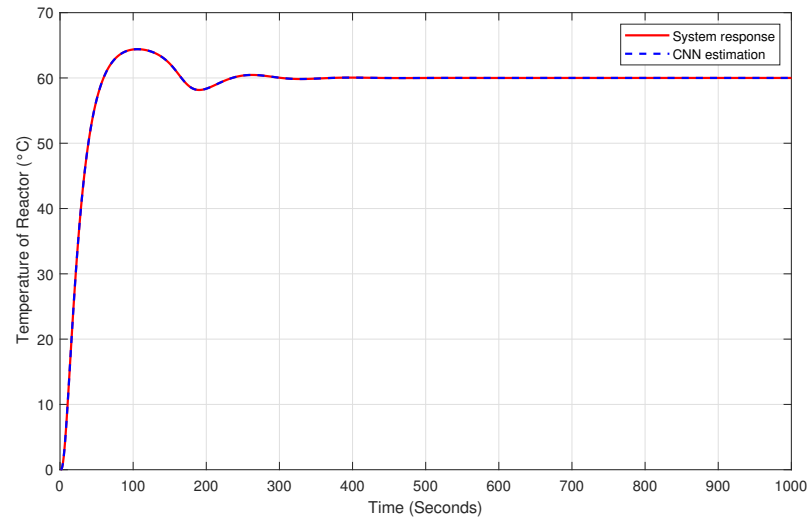
Figure 3. System identification result.

This process can be resumed in Algorithm 1. In it, the first step to propose a CNN structure, i.e., propose the hyper-parameters of the CNN, is performed randomly; there are no specific criteria to chose them. Then, the CNN uses data from the signal U and q_p as input to calculate the estimated value of q_p in that iteration and generate an estimated error, which will be used in the backpropagation algorithm to update the value of the hyper-parameters of CNN. This process is known as the training stage and performed repeatedly until the simulation time is over. Finally, the testing stage is used to verify that the training has been successfully achieved using the MSE metric. If the value of this index is too high, all of the steps are repeated in order to decrease this value.

Algorithm 1 System identification procedure

Propose CNN hyper-parameters, F, NN_W.
while $i \leq N$ **do**   ▷ N -> total of data
    Use control signal U into u_N.
    Run CNN to get $\hat{q}_p$.
    Use system output g_p into u_N for next iteration.
    Compute estimation error $e = \hat{q}_p - q_p$.
    Update hyper-parameters F, N_W using gradient descendant method.
end while
Realize a testing stage to verify the training process with aid of MSE index
if $MSE \geq Mm$ **then**   ▷ Mm -> minimum value for acceptance estimation
    Repeat previous steps with a different CNN hyper-parameters selection.
end if

2.4. Neuro-Fuzzy Controller

The control used in this work is presented in detail in [42]; below is a brief explanation of its operation and mathematical structure. The error (E) and the error increment over time (ΔE) are the inputs necessary for the neuro-fuzzy controller to work. To determine these signals,

$$E(k) = SP(k) - PV(k), \tag{14}$$

$$\Delta E(k) = \frac{E(k) - E(k-1)}{Ts}, \tag{15}$$

where $SP(k)$ and $PV(k)$ denote the set point and the value of the process variable at time k, $E(k-1)$ represents a time delay of $E(k)$, and Ts is the sampling time.

The architecture of NFC is constituted by five layers. The first one, the input vector $X(k) = [E(k), \Delta E(k)]$, is provided for the fuzzification, mapping these real values to the linguistics applied to make the fuzzification according to the Takagi–Sugeno method [43]. The structure of this layer is defined by (16)

$$\mu_{A_{j,k}} = \Gamma_j(\Lambda_j(k), X_i(k)) \tag{16}$$

where $\mu_{A_{j,k}}$ indicates the membership function quantity selected for the vector $X(k)$. Normally, the selection of the number of membership functions is chosen by trial and error, but in this work, it is part of the tuning carried out by a bilevel optimization approach, including the terms related to $\Gamma_j(\cdot)$ and $\Lambda_j(k)$ that describe the j member functions selected to make the fuzzyfication. For the Gaussian bell described by (17), the set $\Lambda_j(k)$ contains the position and the spread of the Gaussian function in the parameters $\phi_{j,k}$ and $\sigma_{j,k}$, respectively [42].

$$\mu_{A_{j,k}}(X_i(k)) = e^{0.5\left(\frac{X_i(k)\phi_{j,k}}{\sigma_{j,k}}\right)^2} \tag{17}$$

The inferences based on the if–then statements are made in the second layer in order to generate fuzzy sets by means of the vector $X(k)$ for subsequent membership in such a way that the functions are related between each other to be able to determine the possible behavior of the system scenarios. Right away, an output value according to each of the cases established by the set of fuzzy rules denoted by (18) is proposed, where the index $p = 2, 3$ corresponds to the second or third layer, respectively [42].

$$O^p = w(k) = \mu_{A_{j,k}}(X_i(k))^T * \mu_{A_{j,k}}(X_i(k)) \tag{18}$$

The output of the third layer should be normalized according to (19), where the index $l = 1, 2, ..., R$ is defined by the number of fuzzy rules n, since $R = n \times n$ [42].

$$\overline{w}(k) = \frac{w(k)}{\sum_{l=1}^{R} w_l(k)} \tag{19}$$

The fourth layer output (O^4) is generated by the products of the normalized firing strength and the parameter $r_l = \gamma_j(\lambda_j(k))$. This value is computed using (20), with $\beta_n(k) \in \Re^n$, $\gamma_j(\lambda_j(k))$ being the membership function and its parameters that describe the controller actions by considering the output of the third layer, and $\overline{w}_{n,:}(k)$ represents each row of the matrix [42].

$$O^4 = \beta_n(k) = \overline{w}_{n,:}(k) * \gamma_j(\lambda_j(k)) \tag{20}$$

The output of the fifth layer is a scalar value used as a control signal that is obtained by (21),

$$U(k) = \sum \beta(k) \tag{21}$$

A hybridization was made with neural networks to give a learning property to the control system, making it able to learn in a continuous way considering the system is subject to different operating conditions such as disturbances, as mentioned in [44]. The gradient descent method [2] was adapted for tuning the membership functions (Gaussians bells) of the neuro-fuzzy network for the fuzzification and defuzzification stages, as shown, respectively, in [42]. This has led to an improvement in the controller that has resulted in an efficient use of energy. However, it can be used to design a desired dynamic for the controller, which can help avoid unwanted actions by the control signal when trying to bring the behavior to a desired set point.

2.5. Sensorless

In biodiesel production, obstacles or situations can be found that make it difficult to control the reactor temperature. The signal emitted by a sensor/transmitter can be corrupted by noise, it can be miscalibrated, and it can fail due to poor installation or lack of maintenance. When any of these situations occur, the controller will be affected due to the dependence on the measurement of the controlled variable to obtain the error signal. This can lead to a loss of energy, instability in the system, and a loss of raw material, and it can also put operators and process equipment at risk. This work presents a solution that allows to attack this problem through the implementation of the CNN as a virtual sensor, which has the purpose of replacing the sensor/transmitter signal in its absence. Below, in Figure 4, it is shown how the CNN acts in the sensorless system. The CNN for this case, which was previously trained to estimate temperature, uses only information from the controller signal, the set point, and the output of itself as input to estimate this variable, so the controller does not obtain a zero at any time, even if the transducer presents any kind of failure.
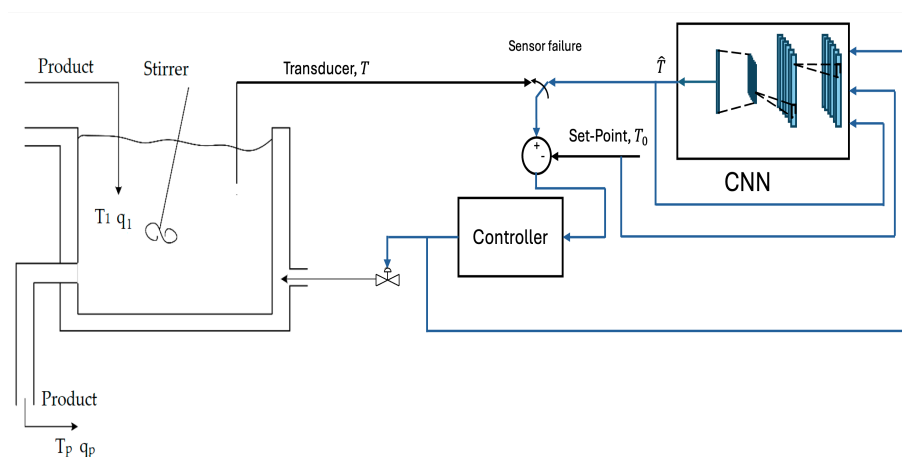

Figure 4. Sensorless system.

In order to show the benefits of the sensorless systems, a simulation was created where the signal from the temperature sensor is missing to compare with real case scenarios where there is a failure in communication with the sensor, such as accidental cable disconnection or breakage. In this case, the controller will send a signal to increase temperature because of the zero signal sent by the sensor, leading to increased energy consumption. For this matter, the plant is controlled with a PID to reach 45 °C with an external disturbance during the simulation. This can be seen in Figure 5; the reactor temperature fluctuations are due to intermittencies in the connection with the sensor. These intermittencies are simulated as occurring repeatedly during certain periods of time in addition to an external disturbance occurring in the system at 5000 s. Both before and after the disturbance, the system will not reach the desired temperature due to the loss of communication with the sensor, potentially compromising the final product properties.

As a solution for this particular problem, a CNN with 2 convolutional layers with 20 filters in each layer and 10 synaptic weights was trained to model the plant and used in parallel with it. In each instance of measurement, the two signals corresponding to the temperature of the reactor can be used as the feedback signal to the controller, preventing the controller from sending an incorrect signal when communication with the sensor is lost, reducing energy consumption and allowing the sensor to be checked without having to stop the process. In both cases, whether the CNN is used or not, 100 s are simulated as the time that the signal sensor is faulty. Figure 6 shows the temperature of the reactor when a

CNN is employed; as it can be seen, the controller takes the system to temperature near the defined set point even though the disturbance appears, unlike the previous case.
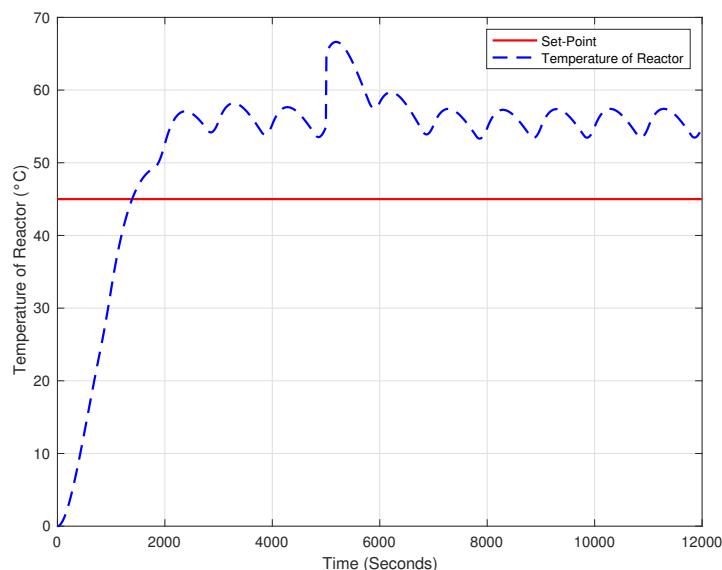

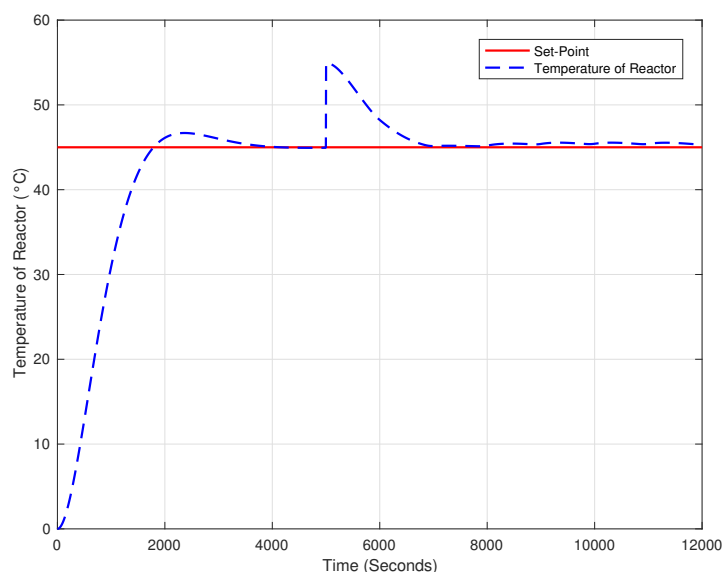**Figure 5.** Temperature of reactor with sensor failure communication.

Figure 6. Temperature of reactor with sensor failure communication using CNN.

2.6. Tuning NFC Parameters with a Bilevel Optimization Approach with Differential Evolution (DE)

In [45], it is explained that the tuning of the NFC controller is complex because the configuration space contains vectors with different dimensions that contain both integers and continuous variables, which is a limitation of implementing search algorithms in order to find the best one. In that work, it was proposed to solve the drawbacks following a bilevel optimization approach, which refers to one in which one problem is embedded within another so that the solution of the first (lower problem) restricts the second (upper problem) [46]. As a contribution to this proposal, the modifications to the bilevel optimization approach are presented to tune the NFC with the objective of covering the additional requirement of not exceeding the reference value of the controller.

2.6.1. The Original Problem

The optimization problem presented in [45] that has the objective of tuning the NFC for the tracking task is described below. For both levels of the methodology, the same objective function presented in (22) is considered where e is determined as the difference between a signal control and the result of applying the NFC to the system.

$$f(\vec{x}) = \sum_{i=1}^{k}(|e_i(\vec{x})| + L|\dot{e}_i(\vec{x})|) \tag{22}$$

In (22), the integers decision variables in $\vec{x}$ are the number of membership functions (m), while the weights of the neural network $[w_1, w_2, ..., w_n]$, the parameters of the membership functions ($\phi_{j,k}$) and ($\sigma_{j,k}$), and the learning rate constants η_ϕ, η_σ and η_r are real-value variables. L is a scalar that serves to regulate the influence of the change in the error as a term of the objective function.

The solution spaces differ in the sense that in the first level, part of the solution is completed with random values; on the other hand, in the second level, the random part becomes the solution to be searched using part of the previously found solution as constants. In the first level of optimization, the weights and the initial position of the member functions are not considered as design variables but as a noise vector, resulting in a solution vector and a noise vector structured as in (23) and (24), respectively.

$$\vec{x} = [m, \sigma_1, \sigma_2, \eta_\phi, \eta_\sigma, \eta_r] \tag{23}$$

$$\vec{w} = [w_1, w_2, \ldots, w_{n=m^2}, \phi_1, \phi_2, \ldots, \phi_m] \tag{24}$$

From (23), it is ensured that the size of the solution vector ($\vec{x}$) is fixed. To complete the configuration of the NFC, the vector is combined with randomly generated sets of weights 10 m^2 in size, where the set with the lowest objective function is selected as the fitness for the solution vector. This solution is carried out around the epochs of the DE as an elitist mechanism. Finally, to deal with the integer value (m), the repulsion strategy proposed by Liu et al. [47] is employed.

At the second level, the solution obtained at the first level of optimization allows establishing a restriction at the second level to make the number of functions and weights constant, where the NFC weights are tuned. The structure of the solution vector for the second level is denoted by (25); m has a fixed size and comes from the previous level as a solution. In this second level of optimization, some elements of the solution vector continue as a decision variable; although weights and positions of member functions are greatly important, it is possible that a different configuration would be better for the tracking task.

$$\vec{x} = [\sigma_1, \sigma_2, \eta_\phi, \eta_\sigma, \eta_r, w_1, \ldots, w_{n=m^2}, \phi_1, \ldots, \phi_m] \tag{25}$$

2.6.2. The Proposed Modified Problems

The tuning methodology was modified as the contribution of this work to integrate the additional requirement of not surpassing the point reference in the tracking task. Two new optimization functions were considered. The first one penalizes the value of the objective function every time the controller's action produces a value that exceeds the reference, as shown in (26).

$$f(\vec{x}) = \sum_{i=1}^{k}(|e_i(\vec{x})| + L|\dot{e}_i(\vec{x})| + M\breve{e}_i(\vec{x})) \tag{26}$$

where M is a scalar that regulates the influence of the new term on the objective function. $\check{e}_i$ defines the error over the set point and is described by (27) using the description of the NFC.

$$\check{e}_i = \begin{cases} \check{e}_i = PV(k) - SP(K), & 0 \leq PV(k) - SP(K) \\ \check{e}_i = 0, & other. \end{cases} \tag{27}$$

This proposal follows the idea presented in [48] where in order to cover multiple objectives, a common objective function is established, which is a composition of different individual functions whose optimal solution involves covering the objective. As the value of M increases, the overreaction is reduced but does not necessarily reach the optimal value of zero. To force the search algorithm to find solutions with that value, a second approach is proposed.

The second proposal consists of biasing the space of feasible solutions by incorporating the constraint (28) to the original objective function (22). The constraint considers a configuration infeasible when it produces system behavior where the controller action exceeds the set point value when the initial condition begins. Due to the incorporation of this restriction, the feasibility rules [49] as a constraint handler were included in DE.

$$h(\vec{x}) = \sum_{i=1}^{k} \check{e}_i(\vec{x}) = 0 \tag{28}$$

The definition of $\check{e}_i$ implies that it can only have positive or zero values, so the solution of the optimization problem represents the best configuration to perform the monitoring task without exceeding the reference.

2.6.3. Final Methodology

The general process for solving the complete optimization problem of the modified approach is shown in Figure 7, and the operations for the mutation, cross, and selection are described by (29), (30) and (31), respectively. All tuned parameters and its range are shown in Table 1.

$$Mutantx^j = x^{r1} + F(x^{r2} - x^{r3}) \tag{29}$$

$$Newx_i = \begin{cases} Mutantx_i, & rand(0,1) \leq CR \\ Fatherx_i, & rand(0,1) > CR. \end{cases} \tag{30}$$

$$x^{g+1} = \begin{cases} Newx_i, & f(Newx_i) \leq f(x^g) \wedge h(Newx_i) = h(x^g) = 0 \\ x^g, & f(x^g) < f(Newx_i) \wedge h(Newx_i) = h(x^g) = 0 \\ Newx_i, & h(Newx_i) \leq h(x^g) \wedge (h(Newx_i) \neq 0 \vee h(x^g) \neq 0) \\ x^g, & h(x^g) < h(Newx_i) \wedge (h(Newx_i) \neq 0 \vee h(x^g) \neq 0) \end{cases} \tag{31}$$

Table 1. Tuned parameters for the NFC.

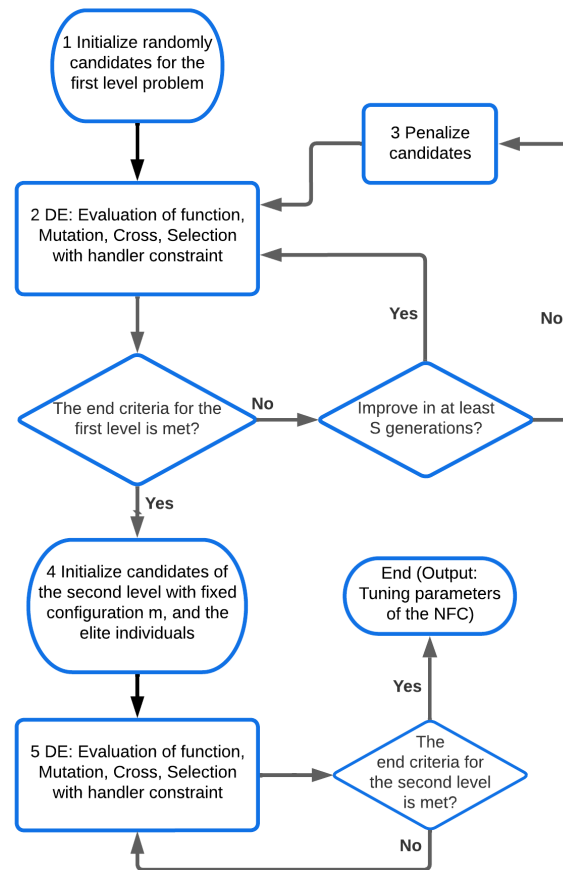| Parameter	Range
Parameter of the membership functions ($\phi_{j,k}$ and $\sigma_{j,k}$)	$\phi_{j,k}, \sigma_{j,k}$ $\in [-100, 100]$
Learning rate constants $\eta_\phi, \eta_\sigma, \eta_r$	$\eta_\phi, \eta_\sigma, \eta_r$ $\in [0.0001, 3]$
Member functions number m	$m \in \mathbb{Z} \cap [3, 15]$
Initial weights $\vec{w}$ refereed to r_j	$w_i \in [0.0001, 50]$

Figure 7. Flowchart of the tuning process.

3. Experimentation and Discussion

3.1. Case of Study

One of the main objectives of biodiesel production is to control the temperature at a desired set point. According to Figure 1, it is possible to perform a heating stage by supplying heat or to carry out a cooling stage, for example, by supplying cold water. When each of the stages occurs, it is due to the nature of the control action determined by the control system based on the temperature variation of the biodiesel production system. One of the main causes that can be easily seen is that if the plant is exposed to an uncontrolled environment, then it is susceptible to environmental factors such as the variation in ambient temperature throughout the day or the season of the year. For example, in the summer, it could be thought that the cooling stage is used more frequently; on the contrary, in the winter, the heating stage could be used more frequently. These environmental variations from the point of view of Automatic Control are considered disturbances. In [45], they are addressed in greater detail. In Section 2.5, it is proposed that the optimization algorithm based on metaheuristics conducts a search and performs a tuning such that the controller in its heating stage mitigates exceeding the desired temperature reference; this leads to energy savings by avoiding the cooling stage being used constantly. Therefore, the above illustrates that considerable efforts can be made to achieve better results from the production processes through not only making improvements in the controller but by making a critical analysis of the needs of a process through understanding it and the industrial objectives.

To illustrate the method proposed in this work, we used the model identified by the CNN. Subsequently, tests were carried out with the proposed functions (26) and (28). The reference of 60 °C was taken; according to the problem posed in [42], at 5000 s, a disturbance due to heat loss of 10 °C is simulated. This may be due to a failure in the control system or

some unexpected external agent that causes such a loss, thus affecting the production of biodiesel. Below is the result obtained by the NFC proposed in [45].

In Figure 8, it is observed that in the initial stage, there is an overshoot, causing the cooling stage of the control system to act to bring the reactor temperature to the desired set point. Later, in the disturbance due to heat demand, it is observed that there is no overshoot in the dynamics of the controlled variable and that the temperature recovery time is gradual.
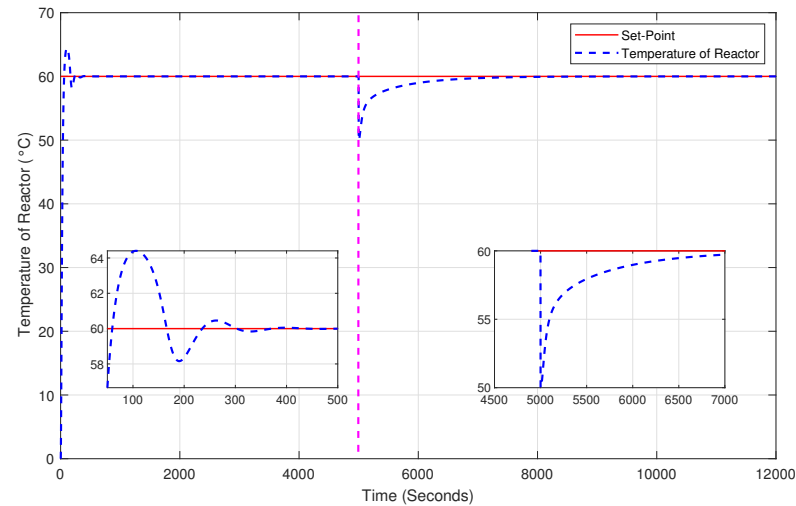

Figure 8. System behavior by NFC without additional considerations.

3.2. First Optimization Proposal

In this experiment, see Figure 9, it is shown how the optimization function proposed in the model (26) penalizes the value of the objective function, as the controller's action produces a value that exceeds the reference. At the beginning of the system response, there is no overshoot, avoiding the cooling stage. However, when the disturbance occurs, it can be observed that in the recovery of the system, there is a time in which the temperature exceeds the proposed reference, so it is necessary to activate the cooling stage. Therefore, speaking in terms of energy savings, it is not desired since this type of system can use cooling towers to supply cold water and lower the reactor temperature.
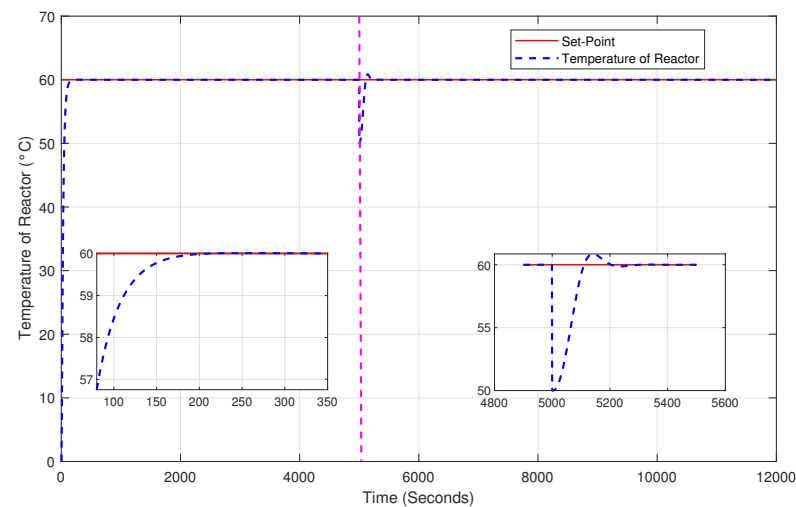

Figure 9. System behavior by NFC with the first optimization proposal.

3.3. Second Optimization Proposal

Figure 10 shows the experimentation considering the second optimization function, which was proposed in model (28), where the constraint considers infeasible a configuration that produces system behavior where the controller action exceeds the set point value when the initial condition begins below. In this case, it is possible to observe that at no time during the experiment, either in the initial stage or at the time of the disturbance, is there a time in which the dynamics of the reactor temperature variable exceed the reference value. Therefore, the activation of the cooling stage was not necessary; this can mean considerable energy savings in biodiesel production systems.
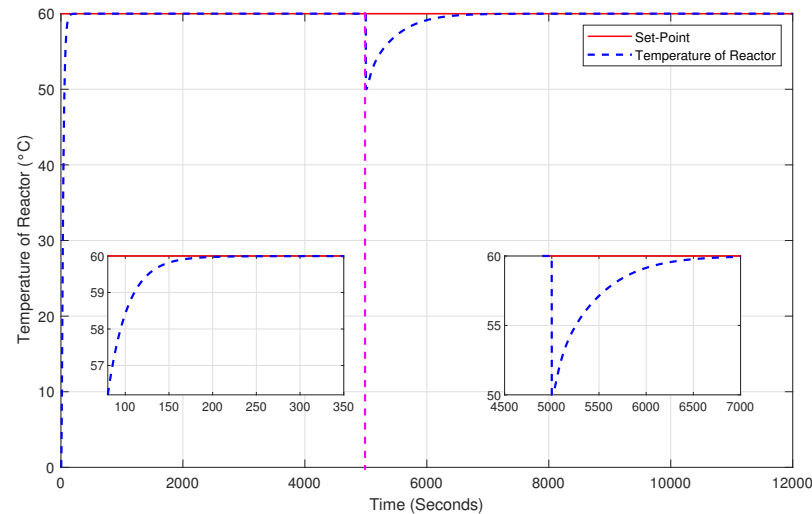

Figure 10. System behavior by NFC with the second optimization proposal.

With this approach, the desired objective was achieved, but due to the stochastic components inherent in metaheuristic techniques, the tuning methodology was repeated 10 times. The results are reported in Table 2. Most of the results are infeasible in the strict sense, but more than half of them have errors less than 1×10^{-6}, so their implementation is viable.

Table 2. Performance of 10 tuned configurations using the second optimization proposal.

Run	Objective Function	Constraint Value	ITAE	TVU
1	8.4832×10^3	0	2.1363×10^7	17.5678
2	5.5300×10^3	10.6989	4.0364×10^6	17.6588
3	4.6494×10^3	3.7802×10^{-5}	4.7453×10^6	30.4145
4	5.3384×10^3	1.9564×10^{-10}	6.2209×10^6	17.5678
5	5.4586×10^3	16.0819	3.8061×10^6	17.7146
6	5.2092×10^3	31.4761	3.3928×10^6	17.9132
7	4.7826×10^3	2.1240×10^{-10}	4.5194×10^6	24.6171
8	5.0259×10^3	31.6624	3.6326×10^6	17.9256
9	4.7149×10^3	8.8660×10^{-5}	4.6459×10^6	29.8925
10	6.9511×10^3	3.1859×10^{-10}	5.6212×10^6	17.5678
Average	5.6143×10^3	8.9919	6.1983×10^6	17.5678
Standard deviation	1.2049×10^3	13.1563	5.4005×10^6	5.3431

3.4. Discussion

The performance metric allows us to interpret the dynamics of the system by quantifying the error signal: the smaller the index, the better the controller performance. There

are a variety of metrics that allow the user to obtain many quantitative properties of the performance of the control of dynamic systems [50]. However, when dealing with the temperature variable, it must be taken into consideration that its dynamics are slow, and it is preferable to penalize more strongly the deviations of the controlled variable with respect to the set point in a steady state or in the presence of disturbances with respect to the transient behavior performance. The ITAE metric results are useful since they penalize the error more strongly as time increases; this is preferable for systems with slow dynamics, such as the temperature of the reactor, where the initial error is usually large. Below is the expression of performance metrics [2]:

$$\int_0^\infty t|e(t)| \, dx. \tag{32}$$

To obtain the results presented, the integral corresponding to the ITAE index was approximated to the form presented in (33)

$$\frac{1}{2} \sum_{k=1}^d ke(k) + (k-1)e(k-1). \tag{33}$$

In many processes, the control signal is an important variable to observe when evaluating the performance of the control system. The TVU index is adequate in this case [2]:

$$\sum_{k=1}^d |u(k) - u(k-1)|. \tag{34}$$

Figures 8–10 are helpful in qualitatively judging the behavior of the reactor temperature variable under NFC control with different considerations. However, this is not an analysis that reveals simple proof that one method is better than another. For a numerical comparison point, Table 3 is presented below, which contains the values obtained in each experiment using the ITAE and TVU performance metrics. Identification, system simulation, and controller tuning through optimization were performed using MATLAB R2020a. We used a computing platform with the following specifications: Intel i7 processor at 3.70 GHz, 16 GB of RAM, and Windows 11 operating system.

Table 3. Comparison of controller performance indexes.

Controller	ITAE	TVU
NFC without penalization	1.9597×10^7	22.3993
NFC first optimization proposal	3.5530×10^6	18.3259
NFC second optimization proposal	3.3928×10^6	17.9132

From Table 3, it can be determined that the best control applied is the NFC considering the restriction proposed in the model (28), demonstrating a lower accumulated ITAE error as well as using 20% less energy with respect to the TVU metric. Applied to an industrial control problem, this could mean profits for the company by making better use of the resources involved in the biodiesel production process.

4. Conclusions

This paper presents a way to apply computer science techniques to solve problems in biodiesel production. This includes a conceptual stage featuring the control objective as well as evaluating the results of an experimental phase. The identification phase of the dynamics of a process, by means of a CNN, is crucial to be able to carry out tests through simulations in order to save time and resources. Since this identification is carried out with

real data from the industrial system, the possible deviation in the implementation in the real world will be drastically minimized, which is of great importance so that advanced control techniques are more easily accepted by the industrial sector. A sensorless technique is also shown, which allows the use of a virtual sensor executed by a CNN and continues with the control of the process while there is no signal from the sensor/transmitter element.

NFC controllers are flexible and allow for the easier mitigation of changes in the environment where the biodiesel plant is located, as well as disturbances that could arise, such as mechanical or electronic failures. The combination of control objectives with metaheuristic algorithms allows the focus of the controllers to meet optimization challenges, as has been shown in this work, by limiting the use of the cooling stage in the temperature control of the reactor. Finally, the quantitative comparison using the TVU and ITAE performance metrics allows the evaluation of the different proposals and determines that for this case study, the NFC with an optimization function that penalizes any control signal that causes the reactor temperature to exceed the desired set point is the best option, thereby achieving a lower error, using lower energy consumption (20% less). The next work is intended to implement these advances in a biodiesel production plant and carry out an energy study of the experimental results. Future work is intended to carry out experimental tests in an industrial pilot plant for the production of biodiesel from cooking oil and to conduct a study of the energy quality of the controller developed in this research.

Author Contributions: M.C.M.-R. and R.L.-M. worked on all the tasks, I.C.-M. and M.A.L.-P. worked on the literature review, M.C.M.-R. and R.L.-M. conducted experimental studies, I.C.-M. and R.T.-E. performed the supervision; all authors analyzed the results. All authors have read and agreed to the published version of the manuscript.

Data Availability Statement: The original contributions presented in the study are included in the article; further inquiries can be directed to the corresponding authors.

Conflicts of Interest: The authors declare no conflicts of interest.

References

1. Borase, R.P.; Maghade, D.K.; Sondkar, S.Y.; Pawar, S.N. A review of PID control, tuning methods and applications. *Int. J. Dynam. Control* **2021**, *9*, 818–827. [CrossRef]
2. Ljung, L. *System Identification Theory for User*; Prentice-Hall: Englewood Cliffs, NJ, USA, 1987.
3. Oluyisola, O.E.; Bhalla, S.; Sgarbossa, F.; Strandhagen, J.O. Designing and developing smart production planning and control systems in the industry 4.0 era: A methodology and case study. *J. Intell. Manuf.* **2022**, *33*, 311–332 . [CrossRef]
4. Schwenzer, M.; Ay, M.; Bergs, T.; Abel, D. Review on model predictive control: An engineering perspective. *Int. J. Adv. Manuf. Technol.* **2021**, *117*, 1327–1349. [CrossRef]
5. Shi, H.; Zhang, L.; Pan, D.; Wang, G. Deep Reinforcement Learning-Based Process Control in Biodiesel Production. *Processes* **2024**, *12*, 2885. [CrossRef]
6. Masera, O.; Rivero, J.C.S. Promoting a Sustainable Energy Transition in Mexico: The Role of Solid Biofuels. *BioEnergy Res.* **2022**, *15*, 1691–1693. [CrossRef]
7. Balance Nacional de Energía: Producción de Energía Primaria. Available online: https://www.gob.mx/sener/articulos/balance-nacional-de-energia-296106 (accessed on 14 June 2022).
8. Orozco-Ramírez, Q.; Cohen-Salgado, D.; Arias-Chalico, T.; García, C.A.; Martínez-Bravo, R.; Masera, O. Production and market barriers of solid forest biofuels in Mexico from the enterprises' perspective. *Madera Bosques* **2022**, *28*, e2812404. [CrossRef]
9. Sosa-Rodríguez, F.S.; Vazquez-Arenas, J. The biodiesel market in Mexico: Challenges and perspectives to overcome in Latin-American countries. *Energy Convers. Manag. X* **2021**, *12*, 100149. [CrossRef]

10. Macías-Alonso, M.; Hernández-Soto, R.; Carrera-Rodríguez, M.; Salazar-Hernández, C.; Mendoza-Miranda, J.M.; Villegas-Alcaraz, J.F.; Marrero, J.G. Obtention of biodiesel through an enzymatic two-step process. Study of its performance and characteristic emissions. *RSC Adv.* **2022**, *12*, 23747–23753. [CrossRef]

11. Boly, M.; Sanou, A. Biofuels and food security: Evidence from Indonesia and Mexico. *Energy Policy* **2022**, *163*, 112834. [CrossRef]

12. Yaqoob, H.; Teoh, Y.H.; Sher, F.; Farooq, M.U.; Jamil, M.A.; Kausar, Z.; Sabah, N.U.; Shah, M.F.; Rehman, H.Z.U.; Rehman, A.U. Potential of waste cooking oil biodiesel as renewable fuel in combustion engines: A review. *Energies* **2021**, *14*, 2565. [CrossRef]

13. Janta-Lipińska, S.; Shkarovskiy, A.; Chrobak, Ł. Improving the Fuel Combustion Quality Control System in Medium Power Boilers. *Energies* **2024**, *17*, 3055. [CrossRef]

14. Ljung, L. Perspectives on system identification. *Annu. Rev. Control* **2010**, *34*, 1–12. [CrossRef]

15. Kozin, F.; Natke, H. System identification techniques. *Struct. Saf.* **1986**, *3*, 269–316. [CrossRef]

16. Nelles, O.; Nelles, O. *Nonlinear Dynamic System Identification*; Springer: Berlin/Heidelberg, Germany, 2020.

17. He, F.; Yang, Y. Nonlinear system identification of neural systems from neurophysiological signals. *Neuroscience* **2021**, *458*, 213–228. [CrossRef]

18. Liu, Y.J.; Zhao, W.; Liu, L.; Li, D.; Tong, S.; Chen, C.P. Adaptive neural network control for a class of nonlinear systems with function constraints on states. *IEEE Trans. Neural Netw. Learn. Syst.* **2021**, *34*, 2732–2741. [CrossRef]

19. Szegedy, C.; Toshev, A.; Erhan, D. Deep neural networks for object detection. In Proceedings of the Advances in Neural Information Processing Systems 26 (NIPS 2013), Lake Tahoe, NE, USA, 5–8 December 2013.

20. Pang, Z.; Niu, F.; O'Neill, Z. Solar radiation prediction using recurrent neural network and artificial neural network: A case study with comparisons. *Renew. Energy* **2020**, *156*, 279–289. [CrossRef]

21. Dolling, O.R.; Varas, E.A. Artificial neural networks for streamflow prediction. *J. Hydraul. Res.* **2002**, *40*, 547–554. [CrossRef]

22. Dong, A.; Starr, A.; Zhao, Y. Neural network-based parametric system identification: A review. *Int. J. Syst. Sci.* **2023**, *54*, 2676–2688. [CrossRef]

23. Lenzi, A.; Bessac, J.; Rudi, J.; Stein, M.L. Neural networks for parameter estimation in intractable models. *Comput. Stat. Data Anal.* **2023**, *185*, 107762. [CrossRef]

24. Liu, Z.; Gao, H.; Yu, X.; Lin, W.; Qiu, J.; Rodríguez-Andina, J.J.; Qu, D. B-spline wavelet neural-network-based adaptive control for linear-motor-driven systems via a novel gradient descent algorithm. *IEEE Trans. Ind. Electron.* **2023**, *71*, 1896–1905. [CrossRef]

25. Derry, A.; Krzywinski, M.; Altman, N. Convolutional neural networks. *Nat. Methods* **2023**, *20*, 1269–1270. [CrossRef] [PubMed]

26. Hubel, D.H.; Wiesel, T.N. Receptive fields of single neurones in the cat's striate cortex. *J. Physiol.* **1959**, *148*, 574–591. [CrossRef]

27. Bharadiya, J. Convolutional neural networks for image classification. *Int. J. Innov. Sci. Res. Technol.* **2023**, *8*, 673–677.

28. Taye, M.M. Theoretical understanding of convolutional neural network: Concepts, architectures, applications, future directions. *Computation* **2023**, *11*, 52. [CrossRef]

29. Krichen, M. Convolutional neural networks: A survey. *Computers* **2023**, *12*, 151. [CrossRef]

30. Fan, G.; Zhang, X. Battery capacity estimation using 10-second relaxation voltage and a convolutional neural network. *Appl. Energy* **2023**, *330*, 120308. [CrossRef]

31. Kabir, S.; Patidar, S.; Xia, X.; Liang, Q.; Neal, J.; Pender, G. A deep convolutional neural network model for rapid prediction of fluvial flood inundation. *J. Hydrol.* **2020**, *590*, 125481. [CrossRef]

32. Rodríguez-Abreo, O.; Velásquez, F.A.C.; de Paz, J.P.Z.; Godoy, J.L.M.; Garcia Guendulain, C. Sensorless Estimation Based on Neural Networks Trained with the Dynamic Response Points. *Sensors* **2021**, *21*, 6719. [CrossRef] [PubMed]

33. Llorente-Vidrio, D.; Ballesteros, M.; Salgado, I.; Chairez, I. Deep Learning Adapted to Differential Neural Networks Used as Pattern Classification of Electrophysiological Signals. *IEEE Trans. Pattern Anal. Mach. Intell.* **2022**, *44*, 4807–4818. [CrossRef]

34. Llorente-Vidrio, D.; Pérez-San Lázaro, R.; Ballesteros, M.; Salgado, I.; Cruz-Ortiz, D.; Chairez, I. Event driven sliding mode control of a lower limb exoskeleton based on a continuous neural network electromyographic signal classifier. *Mechatronics* **2020**, *72*, 102451. [CrossRef]

35. Escobar-Jiménez, R.; Salvide-Hernández, F.; López-Muñoz, R.; Tolentino-Eslava, R.; Maya-Rodriguez, M.C. Monitoring and Prediction of Drinking Water Consumption. In Proceedings of the Telematics and Computing, Cancún, México, 7–11 November 2022; Mata-Rivera, M.F., Zagal-Flores, R., Barria-Huidobro, C., Eds.; pp. 60–75.

36. Pezeshki, Z.; Mazinani, S.M. Comparison of artificial neural networks, fuzzy logic and neuro fuzzy for predicting optimization of building thermal consumption: A survey. *Artif. Intell. Rev.* **2019**, *52*, 495–525. [CrossRef]

37. Pacco, H.C. Simulation of temperature control and irrigation time in the production of tulips using Fuzzy logic. *Procedia Comput. Sci.* **2022**, *200*, 1–12. [CrossRef]

38. Azad, A.S.; Rahaman, M.S.A.; Watada, J.; Vasant, P.; Vintaned, J.A.G. Optimization of the hydropower energy generation using Meta-Heuristic approaches: A review. *Energy Rep.* **2020**, *6*, 2230–2248. [CrossRef]

39. Han, H.; Liu, H.; Li, J.; Qiao, J. Cooperative fuzzy-neural control for wastewater treatment process. *IEEE Trans. Ind. Inform.* **2020**, *17*, 5971–5981. [CrossRef]

40. Stanescu, R.C.; Leahu, C.I.; Soica, A. Aspects Regarding the Modelling and Optimization of the Transesterification Process through Temperature Control of the Chemical Reactor. *Energies* **2023**, *16*, 2883. [CrossRef]

41. Yu, W.; Pacheco, M. Impact of random weights on nonlinear system identification using convolutional neural networks. *Inf. Sci.* **2019**, *477*, 1–14. [CrossRef]

42. Maya-Rodriguez, M.C.; Carvajal-Mariscal, I.; López-Muñoz, R.; Lopez-Pacheco, M.A.; Tolentino-Eslava, R. Temperature Control of a Chemical Reactor Based on Neuro-Fuzzy Tuned with a Metaheuristic Technique to Improve Biodiesel Production. *Energies* **2023**, *16*, 6187. [CrossRef]

43. Bortolet, P.; Palm, R. Identification, modeling and control by means of Takagi-Sugeno fuzzy systems. In Proceedings of the 6th International Fuzzy Systems Conference, Barcelona, Spain, 1–5 July 1997; Volume 1, pp. 515–520. [CrossRef]

44. Huba, M.; Hypiusová, M.; Ťapák, P.; Vrancic, D. Active Disturbance Rejection Control for DC Motor Laboratory Plant Learning Object. *Information* **2020**, *11*, 151. [CrossRef]

45. López-Muñoz, R.; Molina-Pérez, D.; Vega-Alvarado, E.; Duran-Medina, P.; Maya-Rodriguez, M.C. A Bilevel Optimization Approach for Tuning a Neuro-Fuzzy Controller. *Appl. Sci.* **2024**, *14*, 5078. [CrossRef]

46. Dempe, S.; Kue, F.M. Solving discrete linear bilevel optimization problems using the optimal value reformulation. *J. Glob. Optim.* **2017**, *68*, 255–277. [CrossRef]

47. Liu, J.; Wang, Y.; Huang, P.Q.; Jiang, S. Car: A cutting and repulsion-based evolutionary framework for mixed-integer programming problems. *IEEE Trans. Cybern.* **2021**, *52*, 13129–13141. [CrossRef]

48. Starke, S.; Hendrich, N.; Zhang, J. Memetic Evolution for Generic Full-Body Inverse Kinematics in Robotics and Animation. *IEEE Trans. Evol. Comput.* **2019**, *23*, 406–420. [CrossRef]

49. Deb, K. An efficient constraint handling method for genetic algorithms. *Comput. Methods Appl. Mech. Eng.* **2000**, *186*, 311–338. [CrossRef]

50. Dorf, R.C.; Bishop, R.H. *Modern Control Systems*, 14th ed.; Pearson: Boston, MA, USA, 2017.